Hybrid-Resolution Spectral Imaging System Using Adaptive Regression-Based Reconstruction

Keiichiro Nakazaki*, Yuri Murakami, and Masahiro Yamaguchi

Global Scientific Information and Computing Center, Tokyo Institute of Technology,
2-12-1 Ookayama, Meguro-ku, Tokyo, 152-8550 Japan
{nakazaki.k.aa,murakami.y.ac,yamaguchi.m.aa}@m.titech.ac.jp

Abstract. Hybrid-resolution spectral imaging is a technique that efficiently produces high-resolution spectral images by combining low-resolution spectral data with a high-resolution RGB image. In this paper, we introduce a regression-based spectral reconstruction method for this system to enable us doing accurate spectral estimation without a laborious measurement of the spectral sensitivity of the RGB camera. We present two methods for regression-based spectral reconstruction that utilize spatially-registered pair of a low-resolution spectral image and a high-resolution RGB image: whole frame data regression and locally weighted regression. In the experiment, we developed a hybrid-resolution spectral imaging system, and it was confirmed that the regression-based methods can estimate spectra in high accuracy.

Keywords: Spectral Image, Hybrid Resolution Imaging, Regression, Spectral-estimation.

1 Introduction

Spectral image acquisition requires complicated hardware, and usually includes spectral or spatial scanning [1,2,3] or number of image sensors [4]. More sophisticated techniques for spectral imaging have been developed recently [5,6,7], but it is still difficult to capture high-resolution spectral images with a compact device. In order to simplify hardware and to realize one-shot spectral data acquisition, we proposed a hybrid-resolution spectral imaging technique [8, 9], which efficiently produces high-resolution spectral images by combining the data actually measured by two different devices: a low-resolution spectral image and a high-resolution RGB image (Fig. 1). In addition, we developed a low-resolution spectral sensor (LRSS) [9] that captures low-resolution spectral data in one-shot. By using the LRSS accompanied with a commercial color RGB camera, spectral video capture has been realized.

Several methods have been proposed for reconstructing spectral images for hybrid-resolution spectral imaging [8],[10],[11]. Especially piecewise Wiener estimation technique [8] provides significantly better accuracy than conventional techniques and seems to be suitable for hybrid-resolution spectral imaging. However, these methods

* Corresponding author.

A. Elmoataz et al. (Eds.): ICISP 2014, LNCS 8509, pp. 142–150, 2014.

need information of the RGB camera's spectral sensitivity and it affects the accuracy of reconstructed spectral images. Accurate measurement of the spectral sensitivity of a camera requires an other specialized hardware and time-consuming process. In this paper, we introduce a regression-based spectral reconstruction approach [12] to the hybrid resolution spectral imaging system and apply two regression-based spectral reconstruction methods. In the proposed system, it is not required to obtain training data pairs for regression in advance; instead, low-resolution spectral data and high-resolution RGB image are used as training data pairs, and thus real-time processing is possible. In order to introduce a regression-based reconstruction, the registration is required between a low-resolution spectral image and a high-resolution RGB image. Therefore, we also present an automatic registration method based on a template matching.

In the experiment, we developed a hybrid-resolution spectral imaging system in which different spectral estimation methods were implemented for evaluating the reconstructed spectral accuracy. Using the spectral images of a color chart, it was confirmed that the regression-based spectral reconstruction method can estimate spectral reflectance with equivalent or higher accuracy compared to the methods which use the pre-measured sensitivity of the RGB camera. Also the color reproduction under simulated light source was demonstrated.

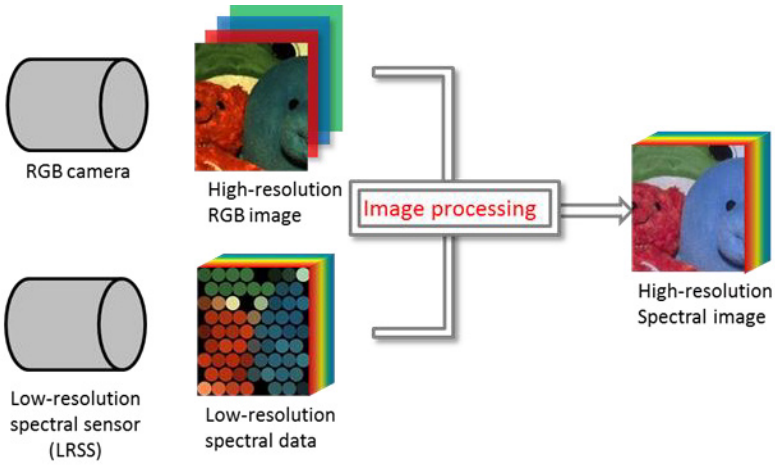

Fig. 1. Conceptual diagram of hybrid-resolution spectral imaging system

2 Hybrid-resolution Spectral Imaging System

The hybrid-resolution spectral imaging system used in this paper consists of a RGB camera (Flea, Point Gray Research, Inc.) of the resolution of 1280×960 pixels and the LRSS [9] which captures 68-pixel spectral radiance image in one-shot in the spectral range 400-780nm The RGB camera and the LRSS are arranged side-by-side to able to shoot the same scene. Fig. 2 shows the photographs of the system. They are connected to a personal computer (PC) through IEEE 1394b interface, which enables

to transfer data to the PC in synchronization. The field of view of the LRSS is smaller than the RGB camera; the area captured by the LRSS corresponds to about 640×720 –pixel area in the RGB image. From the two video streams, spectral image is reconstructed frame by frame. Reproduction of a monochromatic image of arbitrary wavelength or a color image under arbitrary illuminant can be processed in real-time, since the amount of calculation is not very large. It requires only 1×3 or 3×3 matrix multiplication in every pixel, where the matrices are prepared using the LRSS measurement data.

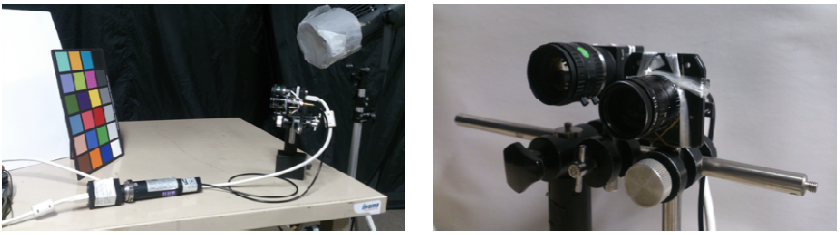

Fig. 2. Photographs of (a) the whole system and (b) the camera head of the hybrid-resolution spectral imaging system

3 Registration between High-Resolution RGB Image and Low-Resolution Spectral Data

To apply multiple regression analysis to the spectral and RGB data captured by those two devices, the image registration is necessary. The registration is accomplished by template matching, but since the high-resolution RGB image and the low-resolution spectral data have different spectral and spatial resolutions, they are not directly used in the matching process. Therefore, firstly a template image is prepared from a frame of low-resolution spectral data, where we use the spatial sensitivity function of LRSS and the scale ratio to high-resolution RGB image. The template image is a RGB image that mimics the spatial sensitivity function of LRSS as shown in left-hand side of Fig. 3. By using this template image, we can find the corresponding region from a high-resolution RGB image (Fig. 3), where rotational shift is assumed to be negligible and the high resolution RGB camera has wider field of view than LRSS does. In this paper, we use normalized cross-correlation for template matching. A correlation coefficient R_{NCC} is calculated as

$$R_{NCC}(i,j) = \frac{\sum_{x=0}^{X}\sum_{y=0}^{Y}\sum_{k=0}^{K-1}\left(I(x+i,y+j,k)-\bar{I}(k)\right)\left(T(x,y,k)-\bar{T}(k)\right)}{\sqrt{\sum_{x=0}^{X}\sum_{y=0}^{Y}\sum_{k=0}^{K-1}\left(I(x+i,y+j,k)-\bar{I}(k)\right)^2 \times \sum_{x=0}^{X}\sum_{y=0}^{Y}\sum_{k=0}^{K-1}\left(T(x,y,k)-\bar{T}(k)\right)^2}}, \quad (1)$$

where T is a template image, I is a high-resolution RGB image, X, Y are width, height of a template image and K is the number of color channels of the high-resolution RGB image. $\bar{T}$ and $\bar{I}$ are the spatial average of T and I.

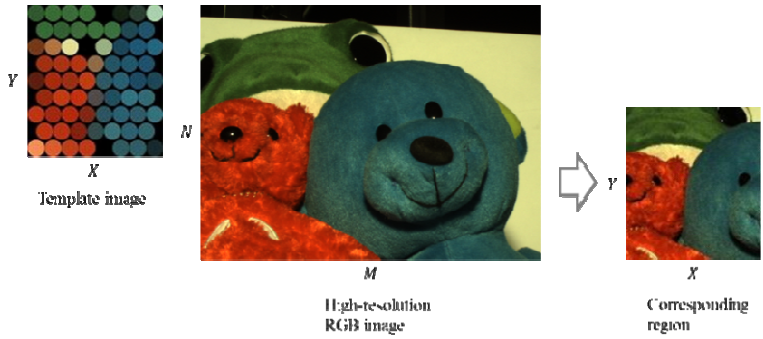

Fig. 3. Template matching

4 Application of Regression-Based Spectral Reconstruction

Through the registration process, we obtain spatially registered low-resolution spectral radiance data and high-resolution RGB images. Based on this data set, a spectral radiance image is reconstructed; we present two regression-based techniques in this paper.

4.1 Full-frame Multiple Regression

In this method, all the corresponding spectral radiance data and RGB data in a frame are used for the multiple regression. Firstly, a low-resolution RGB image is generated from a high-resolution RGB image, where the spatial resolution is equal to low-resolution spectral data. Then, we can obtain multiple pairs of spectral radiance data $\boldsymbol{f}_q$ and RGB signal $\boldsymbol{g}_q(q = 1,2,\dots,Q)$, where Q is the number of the pixels of low-resolution images. Let us define training data matrices $\boldsymbol{G}, \boldsymbol{F}$ as

$$\boldsymbol{G} = \{\boldsymbol{g}_1, \boldsymbol{g}_2, \dots, \boldsymbol{g}_Q\}, \tag{2}$$

$$\boldsymbol{F} = \{\boldsymbol{f}_1, \boldsymbol{f}_2, \dots, \boldsymbol{f}_Q\}, \tag{3}$$

where $\boldsymbol{G}$ is a $K \times Q$ matrix, $\boldsymbol{F}$ is an $L \times Q$ matrix, K is the number of channel of RGB image ($K = 3$ in this case), and L is the number of spectral sampling in low-resolution spectral data. Let $\boldsymbol{G}$ be a set of independent variables and $\boldsymbol{F}$ be a set of dependent variables. Then, a regression coefficient matrix $\boldsymbol{B}$ is calculated as

$$\boldsymbol{B} = \boldsymbol{F}\boldsymbol{G}^t(\boldsymbol{G}\boldsymbol{G}^t)^{-1}. \tag{4}$$

Thus, from a signal of RGB image, we can estimate a spectral radiance function as follows

$$\hat{\boldsymbol{f}}(i,j) = \boldsymbol{B}\boldsymbol{g}(i,j). \tag{5}$$

In this manner, spectra can be reconstructed without the information of spectral sensitivity of the RGB camera, though the derived matrix $\boldsymbol{B}$ contains the information related to the spectral sensitivity of the RGB camera. In addition, in the hybrid-resolution spectral imaging system, we can directly obtain training data for the regression from the target scene. So we can expect high-accuracy in the estimation of spectra.

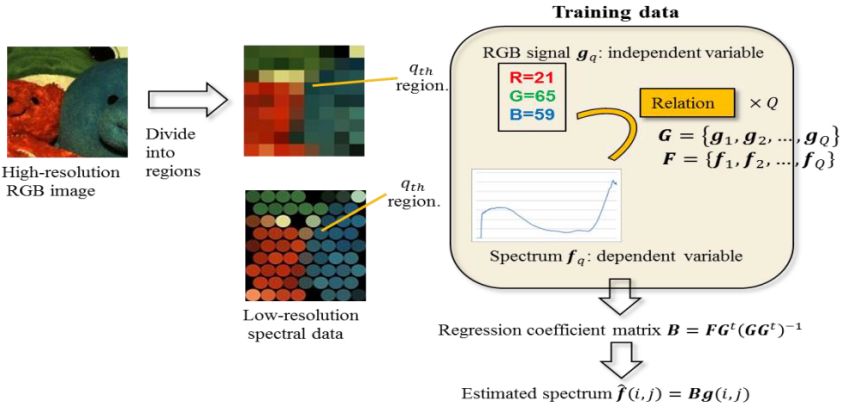

Fig. 4. Multiple regression estimation in hybrid-resolution spectral imaging

4.2 Locally Weighted Multiple Regression

In chapter 4.1, we described a method to calculate a single regression coefficient matrix for a whole image. However, when a variety of objects with different spectral characteristics are included in a frame, the accuracy of estimation is decreased. In this section, we explain a method to derive multiple matrices depending on the positions in the images.

Let us consider to derive regression coefficient matrices per regions corresponding to the pixels of low-resolution images; let $\boldsymbol{M}_q$ be the matrix for qth region. Then, a spectrum of a coordinate (i,j) in the qth region is estimated by using $\boldsymbol{M}_q$. In order to derive $\boldsymbol{M}_q$, we introduce weightings on the data corresponding to qth region and its nearby regions in multiple regression analysis:

$$\boldsymbol{M}_q = \boldsymbol{F}\boldsymbol{A}_q\boldsymbol{g}^t\left(\boldsymbol{g}\boldsymbol{A}_q\boldsymbol{g}^t\right)^{-1}, \tag{6}$$

where $\boldsymbol{A}_q$ is a weighting matrix:

$$\boldsymbol{A}_q = \frac{1}{\sum_{q'=1}^{Q}\alpha_{q,q'}^2}\begin{pmatrix}\alpha_{q,1}^2 & & 0\\ & \ddots & \\ 0 & & \alpha_{q,Q}^2\end{pmatrix}, \tag{7}$$

$$\alpha_{q,q'} = \rho^{d(q,q')}, \tag{8}$$

where $d(q,q')$ is the Euclidean distance between the region q and the region q' and ρ is a scalar parameter that satisfies $0 < \rho < 1$. Thus, the estimated spectral radiance function $\hat{\boldsymbol{f}}(i,j)$ at (i,j)th pixel is calculated as

$$\hat{\boldsymbol{f}}(i,j) = \boldsymbol{M}_q \boldsymbol{g}(i,j). \tag{9}$$

5 Experiments

In order to investigate the accuracy of the regression-based methods applied in the proposed system, we acquired the image of a color chart consisting of four color patches (Fig. 5(a)) and toys (Fig. 5(b)) under an artificial daylight (XC-100AF, SERIC, Inc.). Numbered four areas in Fig. 5(a) and three marked areas in Fig. 5(b) were used for the evaluation. The spectral data were averaged in each area and used to derive the spectral reflectance of the area, where we used the information of the illumination spectra measured by LRSS in advance. In addition, color under CIE D50 illuminant is calculated. The reference data were obtained by measuring respective area by a spectroradiometer (PR650, Photo Research, Inc.).

We compared five methods for spectral image reconstruction: (A) Wiener estimation without the information from the LRSS, (B) Wiener estimation based on the information of LRSS, (C) piecewise Wiener estimation [8], (D) multiple regression, (E) locally weighted multiple regression. The methods (D) and (E) are presented in the chapter 4 of this paper. In the three cases of (A), (B), and (C) pre-measured spectral sensitivity of the RGB camera was used, and spectral images are estimated based on the Wiener theory. In the case of (A), the spectral correlation matrix used in the Wiener estimation was prepared based on Markov model [12], while it was derived from the spectra measured by the LRSS in the case of (B). The method (C) also uses spectral radiance data from the LRSS, but the multiple Wiener estimation matrix is generated per position of the image similar to the method (E).

The estimation results of the spectral reflectance distribution of the area 1 are shown in Fig. 6. From the Fig. 6, we see that the spectral reflectance estimated by a locally weighted regression method is the nearest to the reflectance of all. Table 1 shows the normalized root mean squared error (NRMSE) of spectral reflectance. We can see the NRMSE of locally weighted regression method is significantly smaller than those of other estimation methods. The reason why the locally weighting regression method gives smaller NRMSEs than piecewise Wiener estimation can be considered as the error of the pre-measured spectral sensitivity of RGB camera. If the measurement accuracy of the spectral sensitivity is high enough, the error in the piecewise Wiener estimation is expected to be comparable. It should be noted that the each spectral reflectance function is scaled to have the same integral of the function before calculating NRMSEs and color differences. Fig. 7 shows CIELAB color differences (ΔE) between the true value and the color calculated from the reconstructed spectral reflectance images. We can see that the results by locally weighted regression method are generally better than other methods: the color differences are less or around 5.

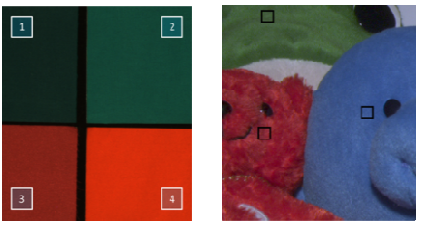

Fig. 5. Spectral images for evaluation (a) color chart and (b) toys

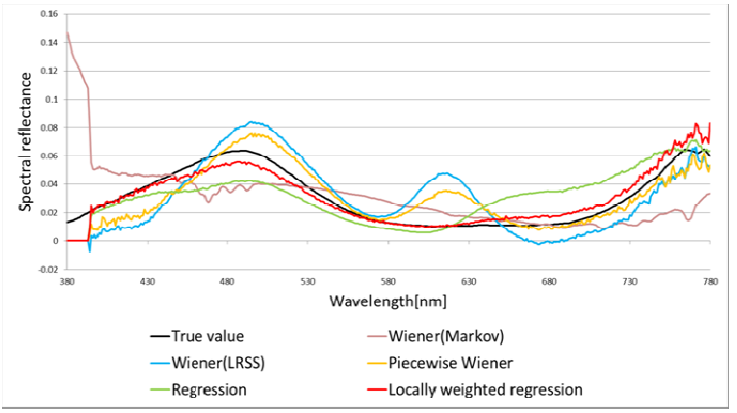

Fig. 6. Reconstructed spectral reflectance of area 1

Table 1. Normalized root mean squared error of spectral reflectance functions [%]

	Wiener (Markov)	Wiener (LRSS)	Piecewise Wiener	Regression	Locally weighted regression
Area 1	48.6	44.7	30.3	39.8	15.6
Area 2	55.5	92.6	16.8	35.3	12.5
Area 3	42.0	10.7	10.6	5.6	5.1
Area 4	40.7	4.5	4.3	4.8	4.6
Red	39.3	4.1	5.1	3.5	5.3
Green	62.4	21.6	15.4	18.5	5.1
Blue	55.1	11.5	12.7	12.8	12.2

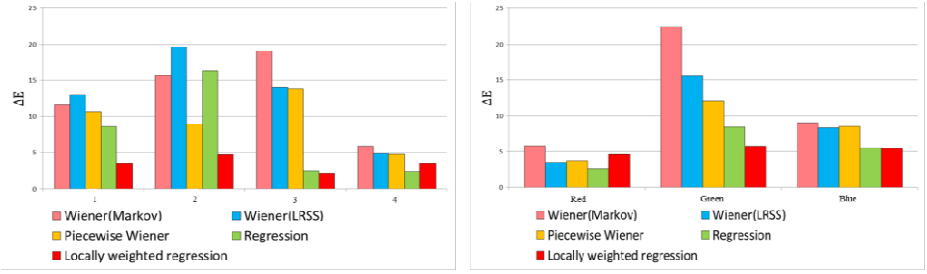

Fig. 7. CIELAB Color difference in (a) a color chart (b) toys under D50 illuminant

6 Conclusions

In this paper, we propose a system for efficient spectral imaging by hybrid-resolution approach utilizing regression-based spectral reconstruction. The proposed method is successfully realized due to the automatic registration method between high-resolution RGB image and low-resolution spectral data. The proposed method enables us to estimate spectral image in high accuracy without using the spectral sensitivity data, thus it will be possible to utilize various off-the-shelf RGB cameras in this system. Also we can combine other spectral images with high-resolution RGB camera to enhance the resolution of the spectral imaging devices.

In the current system, though the registration is not implemented as a real-time process, the remaining processes (capture, reconstruction, and display) work in real-time. It will be possible to increase the processing speed by improving the implementation of the registration process. When utilizing arbitrary RGB cameras, automatic scale fitting between low-resolution and high-resolution data is also required in addition to the spatial registration.

There is a parallax between two cameras in this system. In the experimental system, the distance of two cameras was about 40mm, which was much smaller than the camera-object distance that was about 500mm. Therefore the disparity was very small as compared with the resolution of LRSS, and its influence was almost negligible. However, if the resolution of LRSS will be increased, the influence of the disparity between two cameras should be investigated.

References

1. Hill, B., Vorhagen, W.F.: Multispectral image pick-up system. US Pat. 5319472 (1994)
2. Timo, H., Esko, H., Alberto, D.: Direct sight imaging spectrograph: A unique add-on component brings spectral imaging to industrial application. In: Proc. SPIE, vol. 3302, pp. 165–175 (1998)
3. Richard, M.L., Paul, J.C., Kirill, K.P.: Spectral imaging for brightfield microscopy. In: Proc. SPIE, vol. 4959, pp. 27–33 (2003)
4. Ohsawa, K., Ajito, T., Komiya, Y., Fukuda, H., Haneishi, H., Yamaguchi, M., Ohyama, N.: Six-band HDTV camera system for spectrum-based color reproduction. J. Img. Sci. Tech. 48, 85–92 (2004)
5. Michael, D., Eustace, D.: Computed-tomography imaging spectrometer: Experimental calibration and reconstruction results. Appl. Opt. 34, 4817–4826 (1995)
6. Bedard, N., Hagen, N., Gao, L., Tkaczyk, S.T.: Image mapping spectrometry: Calibration and characterization. Opt. Eng. 51, 111711 (2007)
7. Gehm, M.E., John, R., Brady, D.J., Willett, R.M., Schulz, T.J.: Single-shot compressible spectral imaging with a dual-disperser architecture. Opt. Express. 15, 14013–14027 (2007)
8. Murakami, Y., Yamaguchi, M., Ohyama, N.: Piecewise Wiener estimation for reconstruction of spectral reflectance image by multipoint spectral measurements. Appl. Opt. 48, 2188–2202 (2009)
9. Murakami, Y., Tanji, A., Yamaguchi, M.: Development of Low-resolution Spectral Imager and its Application to Hybrid-resolution Spectral Imaging. In: 12th Congress of the International Colour Association, pp. 363–366. The Colour Group, GB (2013)

10. Murakami, Y., Yamaguchi, M., Ohyama, N.: Class-based spectral reconstruction based on unmixing of low-resolution spectral information. J. Opt. 28, 1470–1481 (2011)
11. Michael, T.E., Russell, C.H.: Hyperspectral Resolution Enhancement Using High-Resolution Multispectral Imagery With Arbitrary Response Functions. IEEE Trans. on Geoscience and Remote Sensing 43, 455–465 (2005)
12. Heikkinen, V., Lenz, R., Jetsu, T., Parkkinen, J., Hauta-Kasari, M., Jääskeläinen, T.: Evaluation and unification of some methods for estimating reflectance spectra from RGB images. J. Opt. 25, 2444–2458 (2008)